ISSN PRINT 2319 1775 Online 2320 7876

*Research paper*  UGC CARE Listed (Group -I) Journal Volume 11, Issue 3, 2019

# Numerical Solution of Hydromagnetic Chemically Reacting and Radiating Casson Fluid Flow Past a Permeable Vertical Stretching Surface

**Bindu.P**[1]

[1]Dept of Engg Mathematics, Koneru Lakshmaiah education Foundation, Green fields, Vaddeswaram, Guntur, India, 52202

**Y. Hari Krishna**[2]

[2]Dept of H&S, ANURAG Engineering College, Ananthagiri, Kodad, Telangana, India-508206

**Abstract:**

In this investigation, we explore the combined effects of a magnetic field, thermal radiation, buoyancy force, viscous dissipation, and chemical reaction on the flow of a Casson fluid over a permeable stretching surface. The nonlinear model equations are formulated and transformed into a set of ordinary differential equations (ODEs). We utilize a shooting technique along with a 6th-order Runge-Kutta iteration scheme to numerically solve the model problem. The results are presented graphically, illustrating the influence of inherent parameters on velocity, temperature, and concentration distributions. Furthermore, the analysis includes tabular presentations of the skin friction coefficient, Nusselt number, and Sherwood number.

**Keywords:** Casson fluid, Prandtl number, bouncy parameter, Eckert number, Heat and Mass transfer

## Introduction

In recent years, there has been a significant focus on investigating the dynamics of Casson fluid flow, as well as heat and mass transfer, over porous stretching surfaces within two-dimensional (2-D) boundary layers. These situations are prevalent in diverse industrial applications, such as polymer processing, paper production, and food manufacturing. The unique properties of non-Newtonian fluids, particularly Casson fluids, in these processes have captured researchers' interest, leading them to explore the behaviors and applications of

ISSN PRINT 2319 1775 Online 2320 7876

Research paper  UGC CARE Listed (Group -I) Journal Volume 11, Issue 3, 2019

these fluids. Boundary layer flows, especially those involving Casson fluid flow over stretching surfaces, have gained importance in aerospace, medical, and fiber production fields. Numerous studies have contributed to the understanding of Casson fluid dynamics. For instance, Eldabe et al. [1] investigated Non-Newtonian Casson fluid flow between rotating cylinders, while Nadeem et al. [2] focused on the magnetohydrodynamic (MHD) flow of a Casson fluid over an exponentially shrinking sheet. Other studies explored various aspects, such as Soret and Dufour effects on MHD flow of Casson fluid [3], Casson fluid flow and heat transfer past an exponentially porous stretching surface [4], and the unsteady radiative-convective boundary layer flow of a Casson fluid with variable thermal conductivity [5]. Researchers have also delved into unsteady free convection flow [6], the influence of a magnetic field on peristaltic flow [7], unsteady MHD free convection flow [8], and heat and mass transfer in magnetohydrodynamic Casson fluid [9]. Recent works [10-25] have addressed heat and mass transfer behavior in magnetohydrodynamic flows involving stretching surfaces. Despite these extensive studies, there exists a noticeable gap in the analysis of Casson fluid flow considering the combined effects of thermal radiation and chemical reaction. This study aims to bridge this gap by numerically investigating Casson fluid flow, heat, and mass transfer over a permeable vertical surface. The investigation considers the influence of a magnetic field, thermal radiation, and chemical reaction effects, employing the shooting method. The study explores the effects of various parameters on fluid velocity, temperature, and concentration profiles. The findings, including friction factor coefficients, as well as heat and mass transfer rates, are presented through graphical representations and tables.

**Model Problem:**

Imagine a stable two-dimensional boundary layer flow of a viscous, incompressible, electrically conducting fluid along a permeable vertical stretching sheet. This sheet is subjected to heat generation, thermal radiation, and a chemical reaction. To induce stretching, two equal and opposite forces are applied along the x-axis, causing the sheet to extend while maintaining the origin fixed, as depicted in Figure 1. Additionally, a magnetic field of uniform strength is applied in the y-direction. It's important to note that the influence of the induced magnetic field is disregarded when compared to the applied magnetic field. The coordinate system is defined with the x-axis along the plate's direction and the y-axis normal to it

ISSN PRINT 2319 1775 Online 2320 7876

Research paper

 UGC CARE Listed (Group -I) Journal Volume 11, Issue 3, 2019

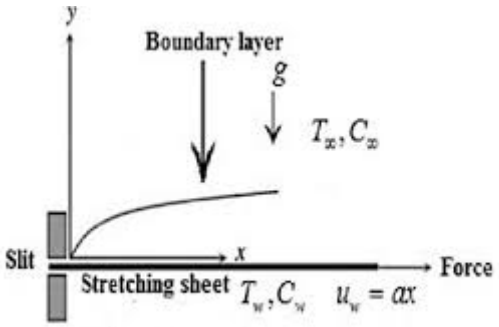


Then the equation of state for an isotropic flow of a Casson fluid is [1]

$$\tau_{ij} = 2\left(\mu_b + \frac{p_y}{\sqrt{2\pi}}\right)e_{ij} \tag{1}$$

where $e_{ij}$ is the $(i,j)^{th}$ component of deformation rate, $\tau_{ij}$ is the $(i,j)^{th}$ component of the stress tensor, $\pi$ is the product of the component of deformation rate with itself, and $\mu_b$ is the plastic dynamic viscosity. The yield stress $P_y$ is expressed as, $P_y = \frac{\mu b\sqrt{2\pi}}{\beta}$ where $\beta$ Casson fluid parameter. For non-Newtonian Casson fluid flow $\mu = \mu_b + \frac{P_y}{\sqrt{2\pi}}$ which gives $\nu' = \nu\left(1+\frac{1}{\beta}\right)$, where $\nu = \frac{\mu b}{\rho}$ is the kinematic viscosity for Casson fluid. It is assumed that plate temperature is initially $T_W$, while the temperature far away the sheet is $T_\infty$. If $u$ and $v$ are the velocity components in $x$ and $y$-directions respectively, then the governing equations for steady boundary layer flow of non-Newtonian Casson fluid are

$$\frac{\partial u}{\partial x} + \frac{\partial u}{\partial y} = 0 \tag{2}$$

$$u\frac{\partial u}{\partial x} + v\frac{\partial u}{\partial y} = \nu\left(1+\frac{1}{\beta}\right)\frac{\partial^2 u}{\partial y^2} + g_0\beta^*\left(T - T_\infty\right) - \frac{\sigma B_0^2}{\rho}u \tag{3}$$

$$u\frac{\partial T}{\partial x} + v\frac{\partial T}{\partial y} = \frac{k}{\rho c_p}\frac{\partial^2 T}{\partial y^2} + \frac{\nu}{c_p}\left(1+\frac{1}{\beta}\right)\left(\frac{\partial u}{\partial y}\right)^2 + \frac{\sigma B_0^2}{\rho c_p}u^2 + \frac{Q_0}{\rho c_p}\left(T - T_\infty\right) - \frac{1}{\rho c_p}\frac{\partial q_r}{\partial y},$$

(4)

$$u\frac{\partial C}{\partial x} + v\frac{\partial C}{\partial y} = D_m\frac{\partial^2 C}{\partial y^2} - Kr\left(C - C_\infty\right) \tag{5}$$

ISSN PRINT 2319 1775 Online 2320 7876

Research paper  UGC CARE Listed (Group -I) Journal Volume 11, Issue 3, 2019

where $g_0$ is the acceleration due to gravity, $\beta^*$ is the volumetric co-efficient of thermal expansion, $\sigma$ is the electric conductivity, $B_0$ is the uniform magnetic field strength, $\rho$ is the fluid density, $c_p$ is the specific heat at constant pressure, $k$ is the thermal conductivity, $Q_0$ is the volumetric rate of heat generation and $q_r$ is the radiative heat flux. Dm is the coefficient of the mass diffusivity, C is the concentration of the fluid, Kr is the chemical reaction parameter,

The corresponding boundary conditions are

$$\left.\begin{array}{ll} u = u_w, v = v_w(x), & T = T_w, C = C_w \quad at\ y = 0 \\ u = 0, & T = T_\infty, \ C = C_\infty \quad as\ y \to \infty \end{array}\right\} \tag{6}$$

where $u_w\, uw$ is the tangential velocity and we consider $u_w = Dx, D(>0)$ is a constant and $v_w$ is the suction velocity.

Using Rosseland approximation for radiation we can get

$$q_r = -\frac{4\sigma^*}{3k'}\frac{\partial T^4}{\partial y} \tag{7}$$

where $\sigma^*$ is the Stefan- Boltzman constant and $3k'$ is the absorption coefficient. Here we consider the temperature difference within the flow is very small such that $T^4$ may be expanded as a linear function of temperature. Using Taylor series and neglecting the higher order terms, we get, $T^4 \cong 4T_\infty^3 T - 3T_\infty^4$. Thus equation (4) implies

$$u\frac{\partial T}{\partial x} + v\frac{\partial T}{\partial y} = \frac{k}{\rho c_p}\frac{\partial^2 T}{\partial y^2} + \frac{\upsilon}{c_p}\left(1+\frac{1}{\beta}\right)\left(\frac{\partial u}{\partial y}\right)^2 + \frac{\sigma B_0^2}{\rho c_p}u^2 + \frac{Q_0}{\rho c_p}(T - T_\infty) + \frac{16\sigma^* T_\infty^3}{3k'\rho c_p}\frac{\partial^2 T}{\partial y^2} \tag{8}$$

The governing equations (3) and (8) can be made dimensionless by introducing the following similarity variables.

$$u = Dxf'(\eta), v = -\sqrt{D\vartheta}\, f(\eta) = y\sqrt{\frac{D}{\vartheta}}, \psi = \sqrt{D\vartheta}\, xf(\eta), \theta(\eta) = \frac{T - T_\infty}{T_w - T_\infty}, \phi(\eta) = \frac{C - C_\infty}{C_w - C_\infty} \tag{9}$$

where $\psi$ is the stream function, $\eta$ is the dimensionless distance normal to the sheet, $\theta$ be the dimensionless temperature, $\phi$ be the dimensionless concentration

Using equation (9) in equations (3) and (8), we get

$$\left(1+\frac{1}{\beta}\right)f''' + ff'' - f'^2 + \gamma\theta - Mf' = 0 \tag{10}$$

ISSN PRINT 2319 1775 Online 2320 7876

Research paper  UGC CARE Listed (Group -I) Journal Volume 11, Issue 3, 2019

$$\left(1+\frac{4}{3}N\right)\theta''+\Pr f\theta'+\left(1+\frac{1}{\beta}\right)Ec\Pr\left(f''\right)^2+MEc\Pr\left(f'\right)^2+\Pr Q\theta=0,$$

(11)

$$\phi''+NSc\left(4f'\phi-f\phi'\right)-ScKr\phi=0 \tag{12}$$

The reduced boundary conditions are

$$\left.\begin{array}{lll} f'=1, & f=f_w, & \theta=1,\phi=1 \quad at\ \eta=0 \\ f'=0, & & \theta=0,\phi=0 \quad as\ \eta\to\infty \end{array}\right\} \tag{13}$$

where $M=\dfrac{\sigma B_0^2}{\rho D}$ is the magnetic field parameter, $\gamma=\dfrac{go\beta_T\left(T_w-T_\infty\right)}{D^2x}$ is the buoyancy parameter, $Q=\dfrac{Q_0}{D\rho c_p}$ is the heat source parameter, $\Pr=\dfrac{\mu c_p}{k}$ is the Prandtl number, $Ec=\dfrac{D^2x^2}{c_p\left(T_w-T_\infty\right)}$ is the Eckert number, $f_w=-\dfrac{v_w}{\sqrt{D\vartheta}}$ is the suction parameter and $N=\dfrac{4\sigma^*T_\infty^3}{kk'}$ is the radiation parameter. $Sc=\dfrac{v_f}{D_m}$ is the Schmidt number, $Kr=\dfrac{K_0L}{C_0U_0}$ is the chemical reaction

Finally, skin friction coefficient $\left(C_f\right)$, local Nusselt number $\left(Nu_x\right)$ and Sherwood number $\left(\mathrm{Re}_x\right)$ can be written as

$$C_f\,\mathrm{Re}_x^{1/2}=\left(1+\frac{1}{\beta}\right)f''(0),\ Nu_x\,\mathrm{Re}_x^{-1/2}=-\left(1+\frac{4}{3}N\right)\theta'(0),\ Sh_x\,\mathrm{Re}_x^{-1/2}=-\phi'(0)$$

(14)

**Numerical Procedure**

The system non-linear differential equations (10)-(12) with the boundary conditions (13) have been solved numerically by shooting technique along with 6$^{th}$order Runge-Kutta iteration scheme with MATLAB package. The step size $\Delta\eta$ = 0.01 is chosen to satisfy the convergence criterion of $10^{-6}$ in all cases. The value of $\eta_\infty$ was found to each iteration loop by $\eta_\infty=\eta_\infty+\Delta\eta$. The maximum value of $\eta_\infty$ to each group of parameters $\beta$, $fw$, $Q$,$M$, $Pr$,Ec and $N$ determined when the value of the unknown boundary conditions at $\eta=0$ not change to successful loop with error less than $10^{-6}$.

ISSN PRINT 2319 1775 Online 2320 7876

Research paper  UGC CARE Listed (Group -I) Journal Volume 11, Issue 3, 2019

## Results and Discussion

The results reveal the influence of various parameters, including the Casson parameter, Bouncy parameter, Magnetic parameter, thermal radiation parameter, Prandtl number, Heat source parameter, Schmidt number, Eckert number, and chemical reaction parameter, on velocity, temperature, and concentration profiles. These effects are presented through graphical illustrations, and additional discussions involve the friction factor, Nusselt number, and Sherwood number, which are provided in tabular form. Throughout the study, numerical results are based on common values, denoted as . Figures 2 to 18 illustrate specific parameter influences on the flow characteristics: Figure 2 depicts the impact of the Casson parameter on the velocity profile, indicating a decrease as the Casson parameter increases due to heightened plastic dynamic viscosity resistance, leading to reduced fluid velocity. Figure 3 illustrates that the velocity boundary layer thickness increases with higher Bouncy parameter values. Figure 4 shows the effect of the thermal buoyancy parameter on concentration, indicating an increase in thermal conductivity with higher thermal buoyancy parameter values. Figure 5 demonstrates the decrease in velocity for higher magnetic field parameter (M) values, attributed to stronger Lorentz force opposing fluid motion. Figure 6 depicts the increase in fluid temperature distribution with higher magnetic field parameter (M) values due to the opposing Lorentz force enhancing thermal conductivity. Figure 7 highlights the increase in concentration boundary layer with an applied magnetic field, although concentration profiles decrease with higher heat source and chemical reaction parameters. Figures 8-10 exhibit the influence of Prandtl number (Pr) on velocity, temperature, and concentration profiles, showing no significant impact on concentration but a decrease in temperature and thermal boundary layer thickness with increasing Pr values. Figure 11 illustrates the increase in velocity with higher heat source parameter (Q) values. Figure 12 presents non-dimensional temperature profiles against η for various heat source parameter (Q) values, showing an increase in temperature profiles with heat generation. Figure 13 demonstrates the increase in concentration with higher heat source parameter (Q) values. Figure 14 shows the influence of Schmidt number (Sc) on flow profiles, indicating a decrease in flow concentration with higher Sc values. Figure 15 illustrates the impact of non-dimensional chemical reaction parameter (Kr) on concentration profiles, showing a decrease in concentration with higher Kr values. Figures 16 and 17 depict the effects of varying thermal radiation parameter (N) on flow temperature and concentration, revealing enhanced

ISSN PRINT 2319 1775 Online 2320 7876

Research paper  UGC CARE Listed (Group -I) Journal Volume 11, Issue 3, 2019

temperature distribution and concentration with increasing N values. Figure 18 illustrates dimensionless temperature and temperature gradient for different Eckert number (Ec) values, indicating increased temperature profiles and boundary layer thickness but a decrease in heat transfer rate with higher Ec values. Varying the Eckert number allows for manipulation of wall temperature distribution.

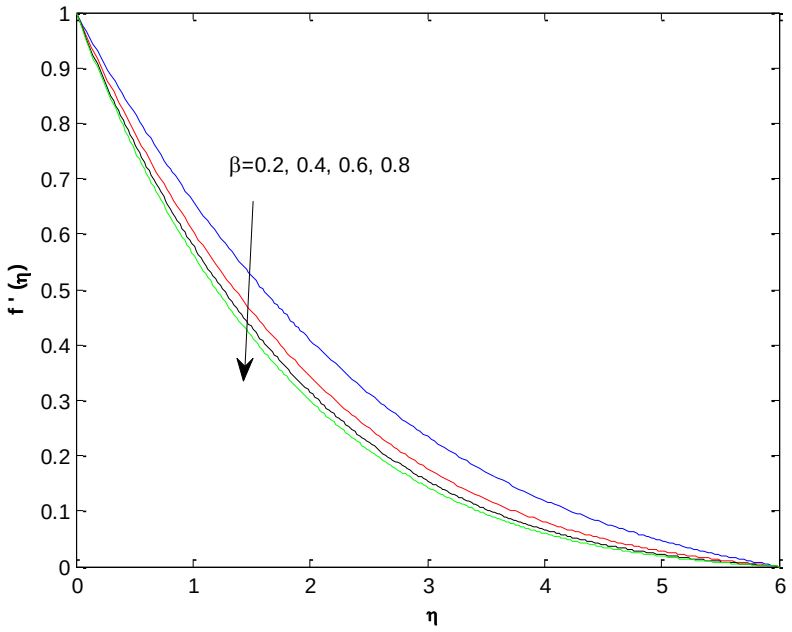


Figure 2: Dominance of $\beta$ on Velocity

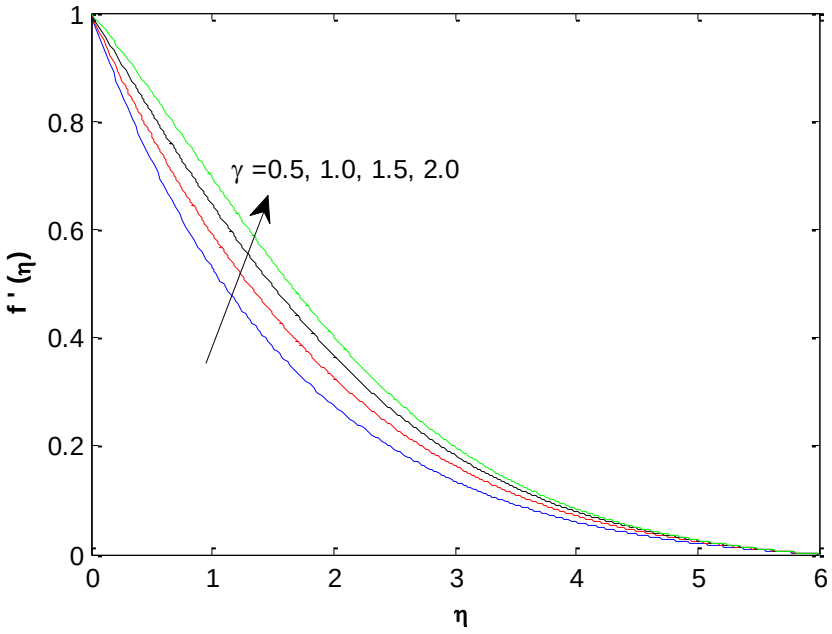

ISSN PRINT 2319 1775 Online 2320 7876

Research paper

 UGC CARE Listed (Group -I) Journal Volume 11, Issue 3, 2019

Figure 3: Dominance of $\gamma$ on Velocity

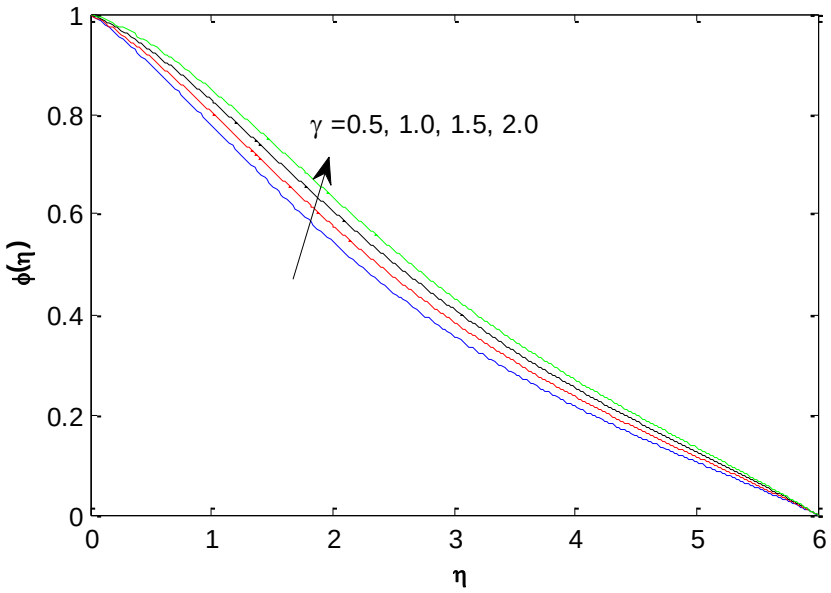


Figure 4: Dominance of $\gamma$ on Concentration

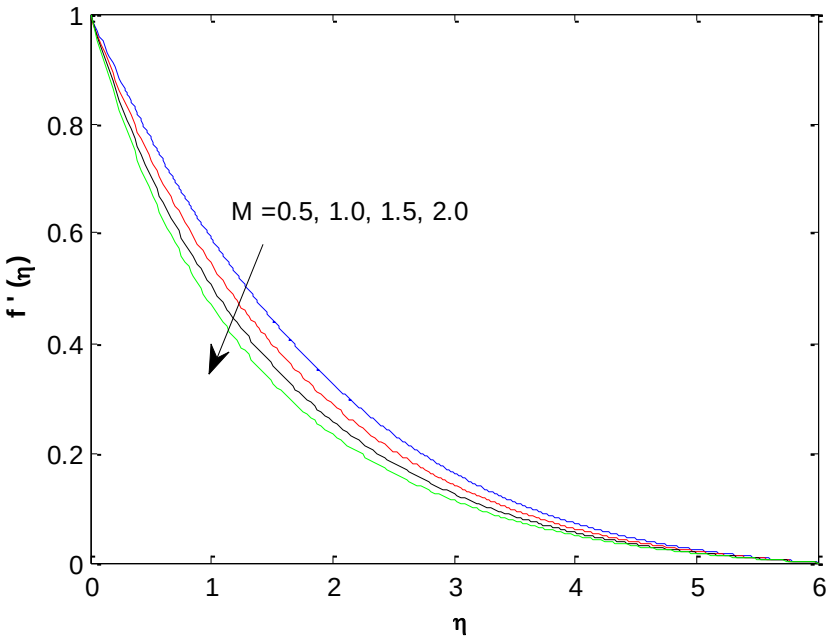


Figure 5: Dominance of M on Velocity

ISSN PRINT 2319 1775 Online 2320 7876

Research paper

 UGC CARE Listed (Group -I) Journal Volume 11, Issue 3, 2019

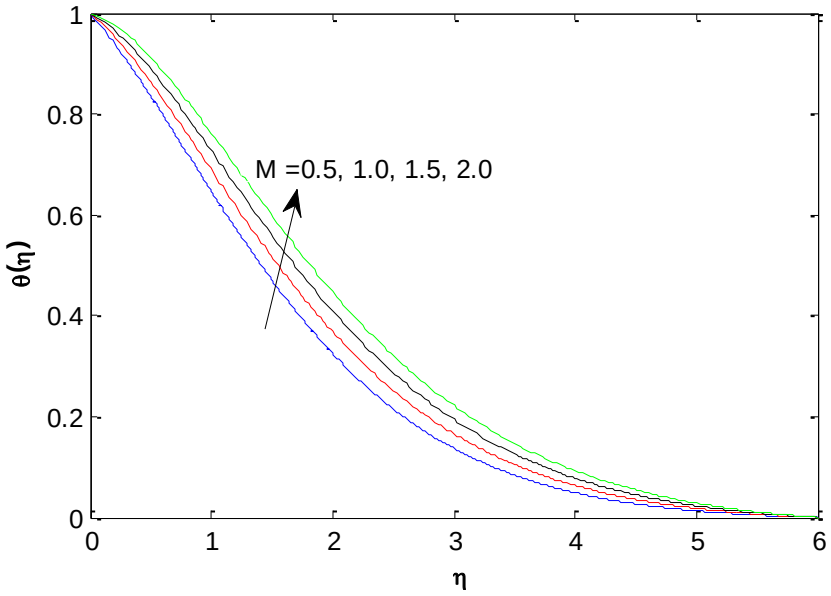


Figure 6: Dominance of M on Temperature

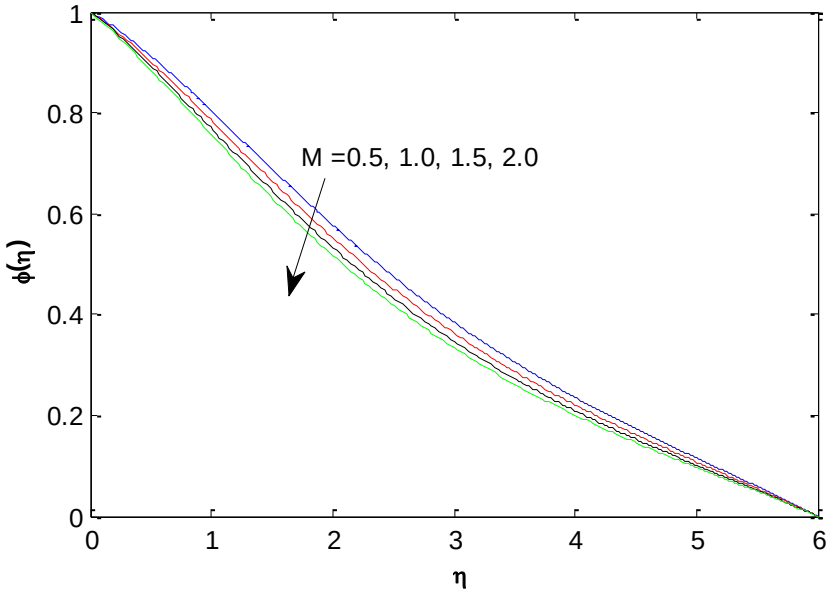


Figure 7: Dominance of M on Concentration

ISSN PRINT 2319 1775 Online 2320 7876

Research paper

 UGC CARE Listed (Group -I) Journal Volume 11, Issue 3, 2019

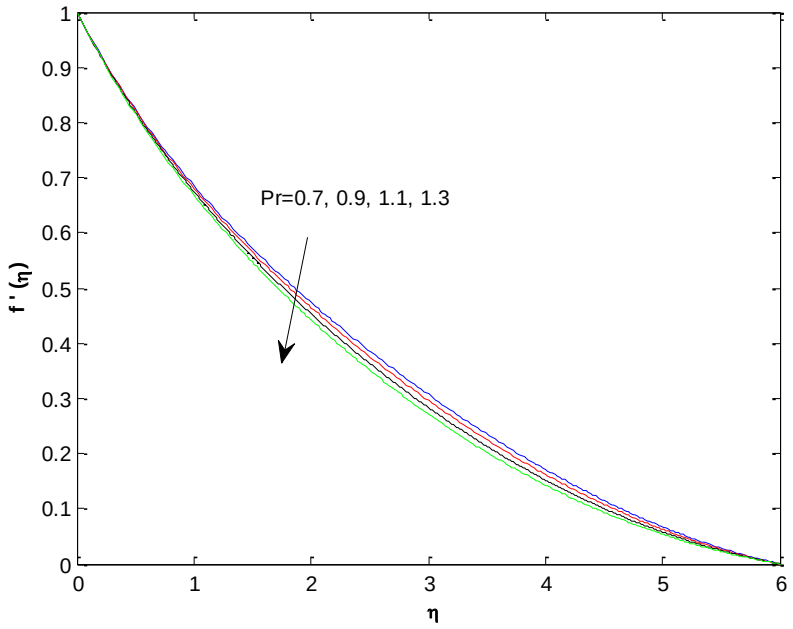


Figure 8: Dominance of Pr on Velocity

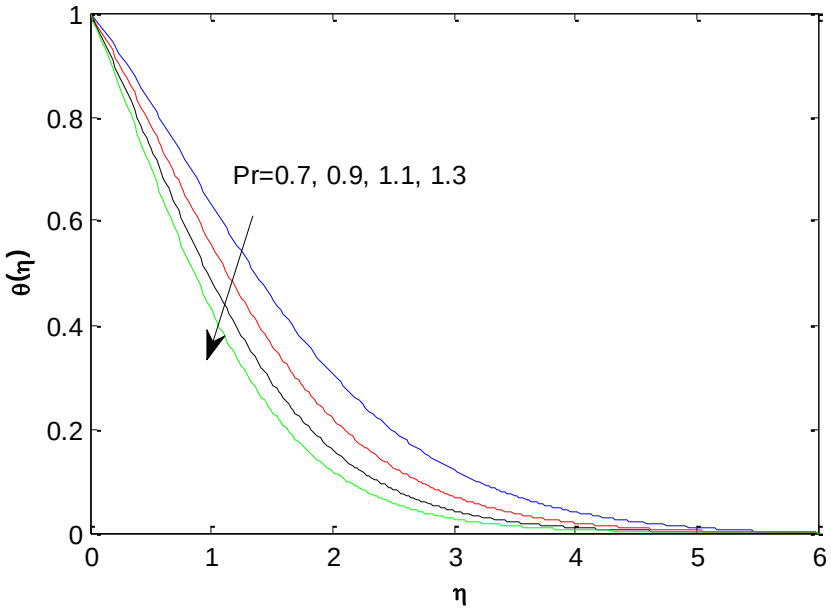


Figure 9: Dominance of Pr on Temperature

ISSN PRINT 2319 1775 Online 2320 7876

Research paper

 UGC CARE Listed (Group -I) Journal Volume 11, Issue 3, 2019

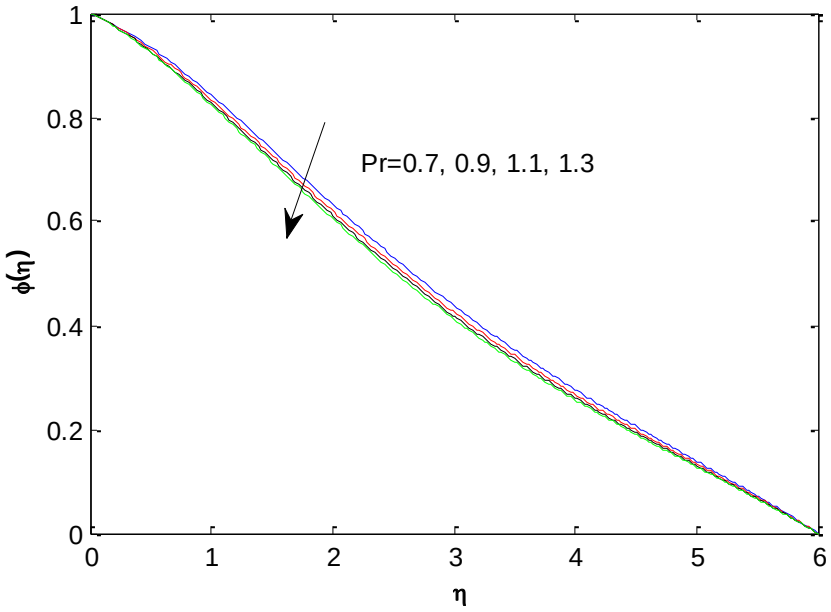


Figure 10: Dominance of Pr on Concentration

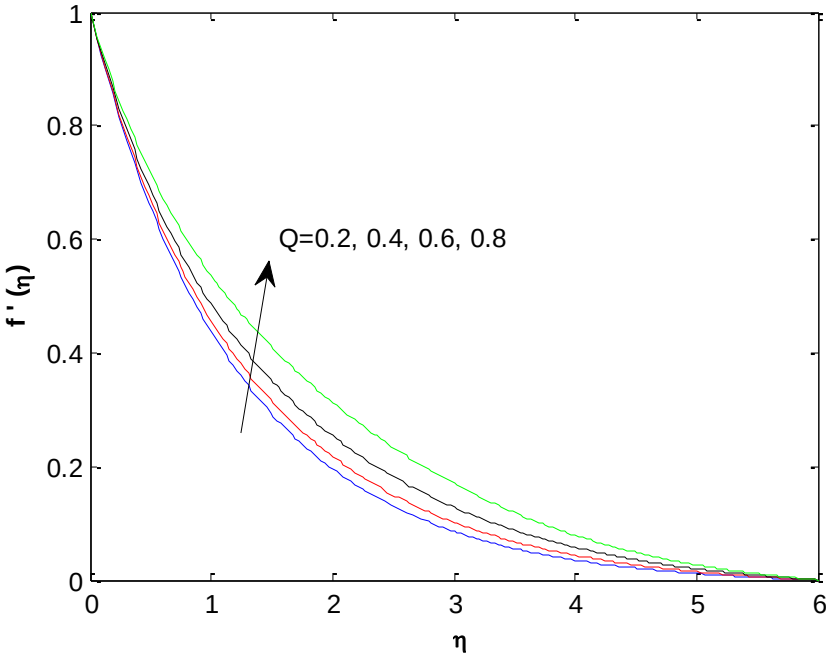


Figure 11: Dominance of Q on Velocity

ISSN PRINT 2319 1775 Online 2320 7876

Research paper

 UGC CARE Listed (Group -I) Journal Volume 11, Issue 3, 2019

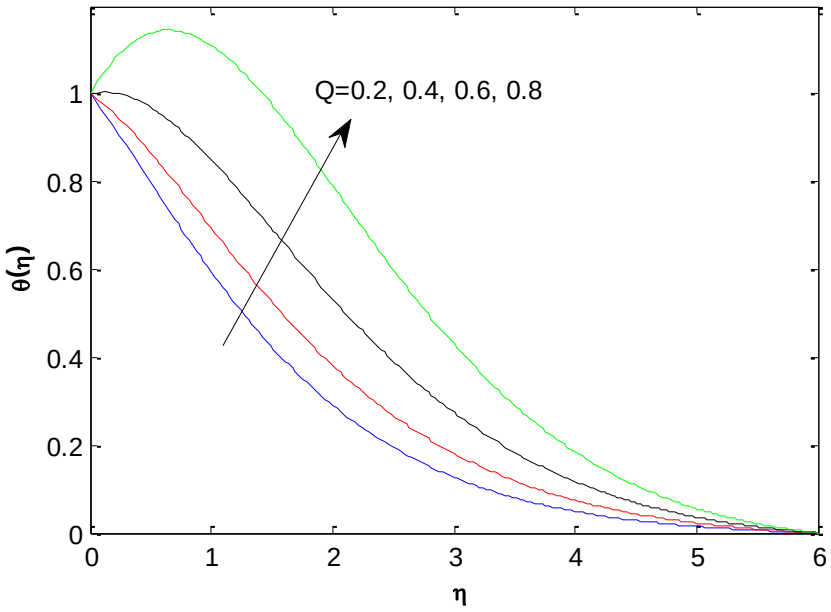


Figure 12: Dominance of Q on Temperature

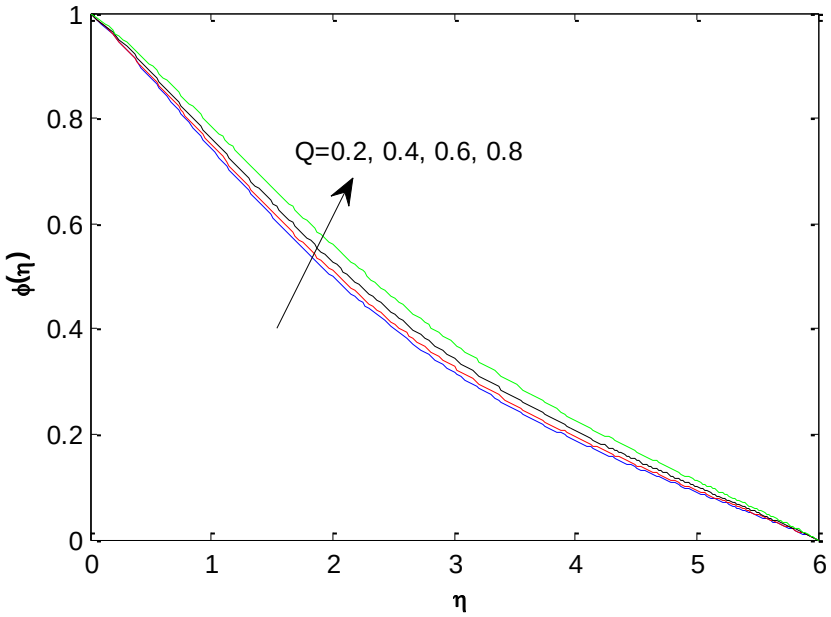


Figure 13: Dominance of Q on Concentration

ISSN PRINT 2319 1775 Online 2320 7876

Research paper

 UGC CARE Listed (Group -I) Journal Volume 11, Issue 3, 2019

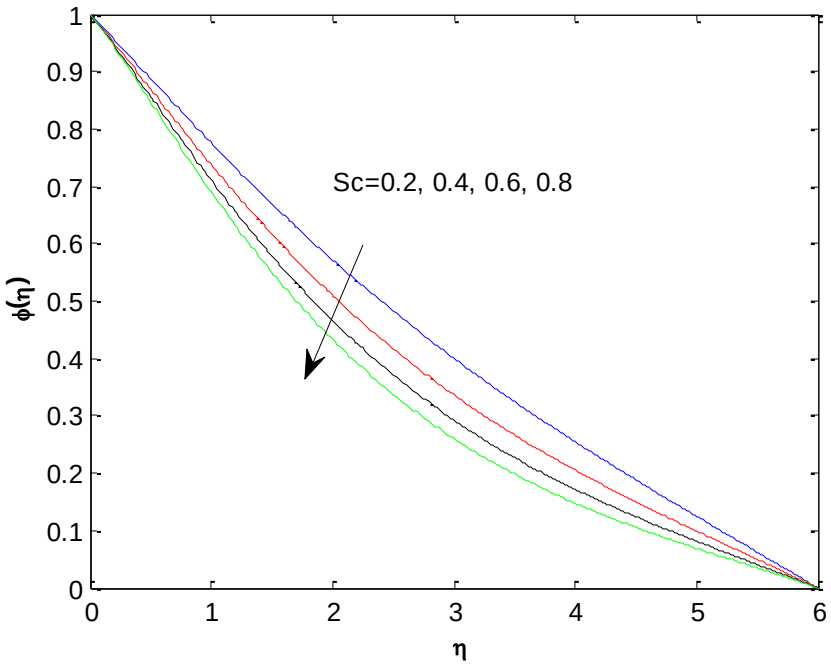


Figure 14: Dominance of Sc on Concentration

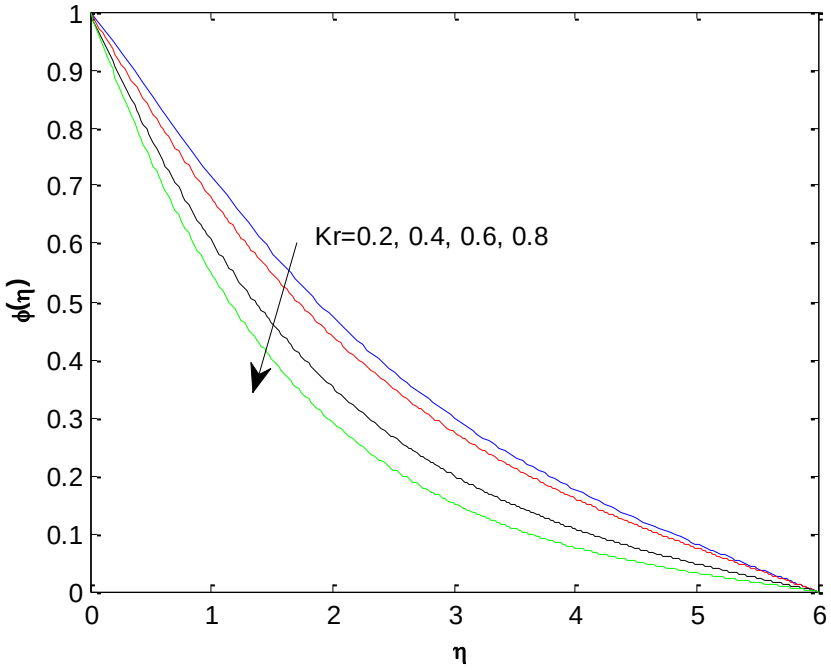


Figure 15: Dominance of Kr on Concentration

ISSN PRINT 2319 1775 Online 2320 7876

Research paper

 UGC CARE Listed (Group -I) Journal Volume 11, Issue 3, 2019

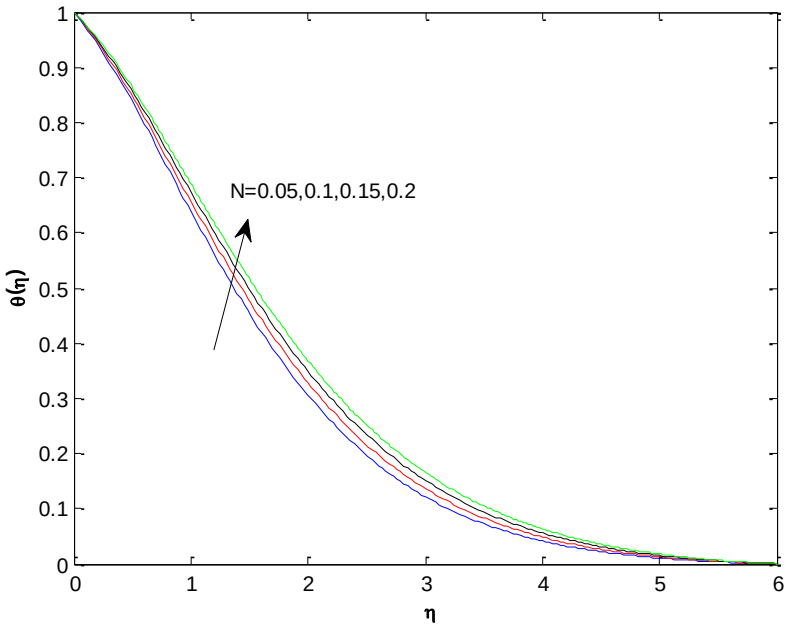


Figure 16: Dominance of N on Temperature

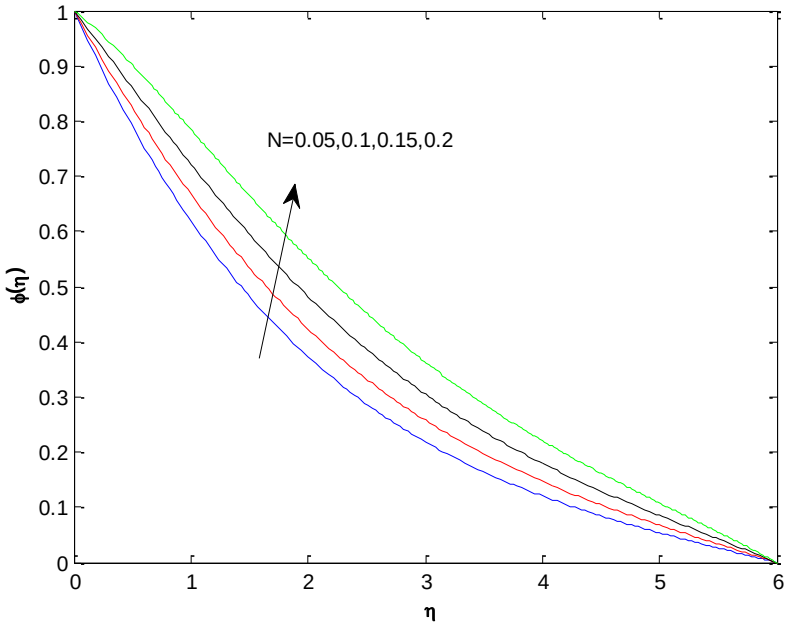


Figure 17: Dominance of N on Concentration

ISSN PRINT 2319 1775 Online 2320 7876

Research paper

 UGC CARE Listed (Group -I) Journal Volume 11, Issue 3, 2019

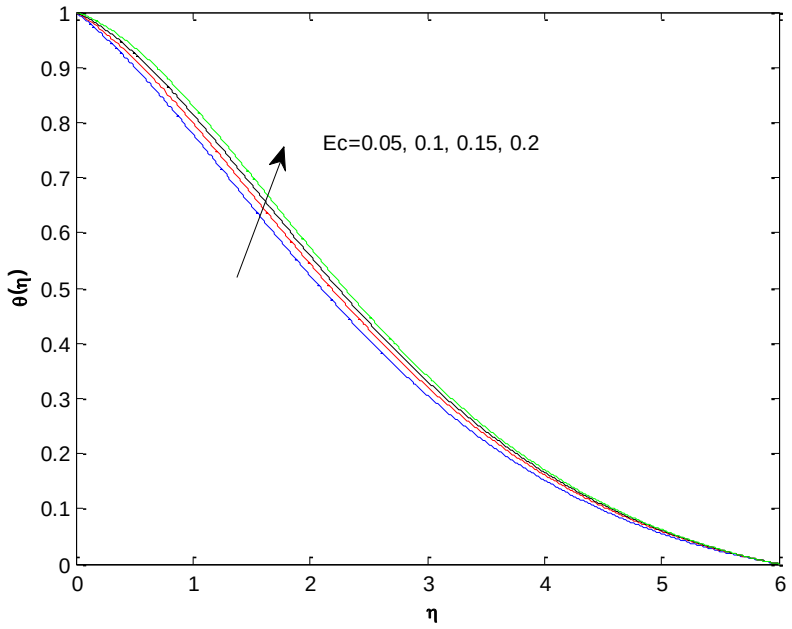


Figure 18: Dominance of Ec on Temperature

**Conclusion**:

This study explores the behavior of Casson fluid over a permeable vertical stretching surface, taking into account the influences of a magnetic field, thermal radiation, and chemical reaction on flow, heat, and mass transfer. The conclusions drawn from the investigation are summarized as follows:

1.Velocity exhibits a decreasing trend with rising values of the Casson parameter, magnetic parameter (M), and Prandtl number (Pr). Conversely, it shows an opposite tendency in the case of the bouncy parameter and heat source parameter (Q).

2.Temperature distribution experiences a decline with an increase in Prandtl number (Pr). In contrast, it demonstrates a reverse tendency in the case of heat source parameter (Q), thermal radiation parameter (N), magnetic parameter (M), and Eckert number (Ec).

3.The concentration boundary layer decreases with an increase in Prandtl number (Pr), chemical reaction parameter (Kr), magnetic parameter (M), and Schmidt number (Sc). Conversely, it exhibits a reverse tendency in the case of thermal radiation parameter (N), heat source parameter (Q), and bouncy parameter.

These conclusions provide insights into the complex interplay of various parameters in the Casson fluid system over a permeable vertical stretching surface, shedding light on the behavior of velocity, temperature, and concentration profiles.

ISSN PRINT 2319 1775 Online 2320 7876

Research paper  UGC CARE Listed (Group -I) Journal Volume 11, Issue 3, 2019

**References**:


1. Eldabe, N. T. M., Saddeck, G. & El-Sayed, A. F. [2001] "Heat transfer of MHD non-Newtonian Casson fluid flow between two rotating cylinders", Mechanics and Mechanical Engineering, Vol. 5, Issue. 2, pp. 237-251.
2. Nadeem, S., Haq, R. U., & Lee, C.[ 2012] "MHD flow of a Casson fluid over an exponentially shrinking sheet," Scientia Iranica, Vol. 19, Issue. 6, pp.1550-1553.
3. T. Hayat, S.A. Shehzad, A. Alsaedi, Soret and Dufour effects on magnetohydrodynamic (MHD) flow of Casson fluid, Appl. Math. Mech. 33 (10) (2012) 1301–1312.
4. S.Pramanik, Casson fluid flow and heat transfer past an exponentially porous stretching surface in presence of thermal radiation, Ain Shams Engineering Journal, Volume 5, Issue 1, March 2014, Pages 205-212
5. M. Gnaneswara Reddy, Unsteady radiative-convective boundary layer flow of a Casson fluid with variable thermal conductivity, J. Eng. Phys. Thermo Phys. 88 (1) (2015) 240–251.
6. A. Khalid, I. Khan, S. Shafiel, Exact solutions for unsteady free convection flow of a Casson fluid over an oscillating vertical plate with constant wall temperature, Abstr. Appl. Anal. (15) (2015) 946350 <http://dx.doi.org/10.1155/2015/946350>.
7. N. Akbar, Influence of magnetic field on peristaltic flow of a Casson fluid in an asymmetric channel: application in crude oil refinement, J. Magnet. Magnet. Mater. 378 (2015) 463–468.
8. A. Khalid, I. Khan, A. Khan, S. Shafie, Unsteady MHD free convection flow of Casson fluid past over an oscillating vertical plate embedded in a porous medium, Eng. Sci. Technol. Int. J. (2015) doi:10.1016/j.jestch.2014.12.006.
9. C.S.K. Raju, N. Sandeep , V. Sugunamma, M. Jayachandra Babu, J.V. Ramana Reddy, Heat and mass transfer in magnetohydrodynamic Casson fluid over an exponentially permeable stretching surface, Engineering Science and Technology, an International Journal 19(2016), 45-52
10. P. BalaAnkiReddy, Magnetohydrodynamic flow of a Casson fluid over an exponentially inclined permeable stretching surface with thermal radiation and chemical reaction Ain Shams Engineering Journal Volume 7, Issue 2, June 2016, Pages 593-602

ISSN PRINT 2319 1775 Online 2320 7876

Research paper  UGC CARE Listed (Group -I) Journal Volume 11, Issue 3, 2019

11. Raju, C. S. K., Sandeep, N., Sugunamma, V., Babu, M. J., & Reddy, J. R. [2016] "Heat and mass transfer in magnetohydrodynamic Casson fluid over an exponentially permeable stretching surface", Engineering Science and Technology, an International Journal, Vol. 19, Issue. 1, pp. 45-52.
12. Reddy, R. C., Reddy, K. J., & Ramakrishna, K. (2016). Effects of joule heating on MHD free convective flow along a moving vertical plate in porous medium. Special Topics and Reviews in Porous Media, 7(2), 207-219. doi:10.1615/SpecialTopicsRevPorousMedia.2016017247
13. Reddy, G. V. R. (2016). Soret and Dufour effects on MHD free convective flow past a vertical porous plate in the presence of heat generation. International Journal of Applied Mechanics and Engineering, 21(3), 649-665. doi:10.1515/ijame-2016-0039
14. Mangathai, P., Ramana Reddy, G. V., & Rami Reddy, B. (2016). MHD free convective flow past a vertical porous plate in the presence of radiation and heat generation. International Journal of Chemical Sciences, 14(3), 1577-1597.
15. Ramana Reddy, G. V., Bhaskar Reddy, N., & Chamkha, A. J. (2016). MHD mixed convection oscillatory flow over a vertical surface in a porous medium with chemical reaction and thermal radiation. Journal of Applied Fluid Mechanics, 9(3), 1221-1229.
16. Ramana Reddy, G. V., Bhaskar Reddy, N., & Gorla, R. S. R. (2016). Radiation and chemical reaction effects on MHD flow along a moving vertical porous plate. International Journal of Applied Mechanics and Engineering, 21(1), 157-168. doi:10.1515/ijame-2016-0010
17. P.Suresh, Y. Hari Krishna, R. Sreedhar Rao, P. V. Janardhana Reddy; "Effect of Chemical Reaction and Radiation on MHD Flow along a moving Vertical Porous Plate with Heat Source and Suction", International Journal of Applied Engineering Research, 14(4), 869-876, 2019
18. BalajiPrakash, G; Reddy, GV Ramana; Sridhar, W; Krishna, Y Hari; Mahaboob, B; Thermal Radiation and Heat Source Effects on MHD Casson Fluid over an Oscillating Vertical Porous Plate, Journal of Computer and Mathematical Sciences,10(5),1021-1031,2019
19. P.Suresh, Y. Hari Krishna, Mahaboob, Amaranath: Heat Transfer and Stagnation Heat Stagnation-Point Flow of Non-Point Non-Newtonian Casson Fluid over Stretching

ISSN PRINT 2319 1775 Online 2320 7876

*Research paper*  UGC CARE Listed (Group -I) Journal Volume 11, Issue 3, 2019

Surface Fluid Surface, International Journal of Modern Engineering and Research Technology, Volume 6 | Issue 2 | April 2019,33-39

20. N Vijaya, Y Hari Krishna, K Kalyani, GVR Reddy Non-Aligned Stagnation Point Flow of a Casson Fluid past a Stretching Sheet in a Doubly Stratified Medium, « Fluid Dynamics & Materials Processing, vol.15, no.3, pp.233-251, 2019